5

Chapter 5

Control of pellet morphology by altering the timing of *matAB* transcription

van Dissel, D., & van Wezel, G.P.

ABSTRACT

The filamentous lifestyle of *Streptomyces* species limits the efficiency of submerged fermentations. Depending on the strain and culturing conditions, streptomycetes grow either as dispersed mycelia or as aggregated pellets during fermentation. Dispersed mycelia are characterized by faster growth, but also by higher viscosity, which negatively affects culture rheology. Pellets hardly affect the viscosity, but in turn are associated with slow growth and prolonged fermentation time. Here, we applied the Ostwald–de Waele power law model to compare rheology and growth of the pellet-forming *Streptomyces lividans* and its *matAB* mutant, which fails to produce the pellet-inducing poly-*N*-acetylglucosamine (PNAG). To create a strain with fast growth and better rheology, we placed *matAB* under the control of two different promoters that are transcribed later during growth, so as to activate aggregation at the end of the exponential growth phase. The recombinant strains showed more aggregation and resulted in up to eight times lower biomass-specific viscosity than the *matAB* mutant, whilst maintaining the 60% faster growth rate compared to wild type *S. lividans*. This is a step towards the best of both worlds, namely a production host that has a high maximum growth rate, whilst limiting the increase in viscosity typical of dispersed mycelia.

INTRODUCTION

Streptomyces are industrial bacteria that produce the majority of naturally occurring antibiotics, numerous anti-cancer compounds and a wide range of industrially relevant enzymes (Barka *et al.*, 2016, Bérdy, 2005, Hopwood, 2007). In contrast to most prokaryotes this phylum grows as multicellular filaments (Claessen *et al.*, 2014). Their filamentous life style negatively influences the rheology during industrial fermentation (van Dissel *et al.*, 2014). Especially high biomass concentrations lead to an enormous increase of the apparent viscosity, and hence a decrease in mixing efficiency, while lowering the oxygen transfer rates and increasing shear forces and thus cell lysis (Wucherpfennig *et al.*, 2010). This potentially results in a decrease in productivity, especially during large scale fermentation, which generally has lower agitation intensities (van't Riet & Tramper, 1991). The extent to which the rheology is altered is highly dependent on the morphology. In particular mycelia growing as loose or dispersed filaments, also referred to as mycelial mats, may lead to tremendous increase in the viscosity as a result of hyphal entanglement, resulting in a culture composition with non-Newtonian characteristics (Metz *et al.*, 1979).

Besides dispersed growth, many *Streptomyces* species aggregate into self-immobilized biofilms, typically referred to as pellets. Pellets do not significantly influence the viscosity, and measurements with filamentous fungi showed that pellets only induce pseudoplastically at very high biomass concentrations (Kim *et al.*, 1983). Although pellets have better rheological properties, a pellet's structure is tightly compacted, thereby restricting mass transfer towards the center. This decreases the overall substrate uptake rate and maximum achievable growth rate, often affecting product yield (van Dissel *et al.*, 2015, Olmos *et al.*, 2013).

Streptomyces lividans, which is considered the preferred *Streptomyces* strain for heterologous enzyme production (Anné *et al.*, 2012), natively grows as dense pellets, but certain morphogenes are known through which it is possible to drastically change this native liquid morphology (van Wezel *et al.*, 2006, Chaplin *et al.*, 2015, van Dissel *et al.*, 2015, Koebsch *et al.*, 2009, Petrus *et al.*, 2016). We recently reported on the discovery of the *matAB* locus, which is required for pellet formation (van Dissel *et al.*, 2015). Removal of the *mat* genes created a strain with a dispersed morphology, increasing the maximal growth rate and the enzyme production rate by over 60%.

To better control *Streptomyces* morphology, with the goal to increase its industrial exploitation, we aimed at optimizing the expression level and timing of the *mat* locus. To this end, the *matAB* genes were expressed from different promoters which activate transcription during late growth. Selecting a promoter which is not active during early exponential growth, but highly expressed in a later growth phase, resulted in a strain with a high initial growth rate, but with reduced viscosity increase seen with a dispersed phenotype. This represents a significant advance in the control of *Streptomyces* morphology and with that potentially also in the applicability of members of this genus in industry.

MATERIALS AND METHODS

Strains, Plasmids and strain construction

Streptomyces lividans 66 was obtained from the John Innes Centre strain collection. its genome was sequenced previously (Cruz-Morales *et al.*, 2013). *E. coli* JM109 was used as host for general cloning (Sambrook *et al.*, 1989). Non-methylating *E. coli* strain ET12567 (MacNeil *et al.*, 1992) harboring plasmid pUZ8002 was used for conjugation of different vectors from *E. coli* to *S. lividans*. *Streptomyces* techniques were performed as described (Kieser *et al.*, 2000). The native *matAB* locus was PCR-amplified from the *S. coelicolor* genome using primers SCO2963_F and SCO2962_R (Table S1). The 3712 bp DNA fragment was cloned as an EcoRI/BamHI fragment into the integrative vector pSET152 (Bierman *et al.*, 1992). The region was >99% homologues to the locus in *S. lividans*. The promoter regions of SCO1800 (P^{chpE}), SCO1947 (P^{gapA}) and of SCO1968 (P^{glpQ2}) were amplified from the *S. coelicolor* genome and ligated into EcoRV-digested pJET1.2. The different promoters were cloned EcoRI/ NdeI in front of *matAB*, creating pMAT6 (pSET152-P^{glpQ2}*matAB*), pMAT7 (pSET152-P^{gapA}*matAB*) and pMAT8 (pSET152-P^{chpE}*matAB*) (Table S2). These vectors were transformed to *E. coli* ET12567 + pUZ8002, which allowed conjugation of these vectors to *S. lividans* Δ*matAB* (GAD5), creating recombinant strains PXM1 (GAD5 + pMAT8), PXM2 (GAD5 + pMAT6) or PXM3 (GAD5 + pMAT7) (Table S2).

Culturing conditions

All *Streptomyces* strains were cultivated in tryptic soy broth medium (TSB). Fermentations were performed in 1.3 L benchtop bioreactors (Bioflow 115, New Brunswick) in duplicate. 900 mL TSB medium was supplemented with 0.1% antifoam. The medium was aerated at 0.5 vvm and the temperature was kept constant at 30^0C. Dissolved oxygen concentrations were kept above 50% by controlling the agitation rate between 300-800 rpm. Concentrations of CO_2 and O_2 were measured in the off gas with an EX2000 gas analyzer (New Brunswick). The dry weight was determined by measuring the differential weight increase of a pre-weighted glass fibre filter disc on which a known culture volume was deposited, washed with at least two volumes demineralized water and followed by freeze drying. Dry weight values were used to calculate growth rates.

Determining the rheology

Viscosity measurements were performed with a DV-E viscometer (Brookfield, USA). A helical impeller, more suited for the measurement of pellet particles in a solution (Kim *et al.*, 1983), was used for measurements. The impeller had a diameter of 23 mm, 36 mm height and 24 mm pitch and was calibrated similarly as described by (Kim *et al.*, 1983) using a series of sucrose concentrations ranging from 70% to 60% and comparing the torque and viscosity values found with a traditional cylindrical spindle. Similar to (Kim *et al.*, 1983) the deviation between the different impeller types was constant in terms of changes in viscosity or torque

and shear rate.

The non-Newtonian behavior of mycelia was described according to the Ostwald–de Waele power law (Metz *et al.*, 1979). The consistency index (K) and the power law index (n) were calculated from the viscosity (η) and shear rate (γ) measurements according to:

$$\eta = K\gamma^{n-1}$$

Biomass specific viscosity index was determined as described by (Riley *et al.*, 2000):

$$\frac{K}{C_X^{\,n}}$$

with C_X being the dry weight biomass concentration and K and n being the values of the power law. Each sample was measured at several shear rates. Because of limitations inherent to the viscometer it was not possible to measure samples with a viscosity below 10 cp, *i.e.* the combination of low biomass and dense pelleting phenotype, and the power law was only fitted when the viscosity of at least four shear rate measurements could be accurately measured. The obtain higher biomass concentrations, in order to establish the relation between pellets and dispersed mycelia, 24h cultures were concentrated by centrifugation at 3000g for 20min and resuspended in fresh media.

Image analysis

Image analysis of S*treptomyces* mycelia was performed as described (Willemse *et al*., unpublished). In short, a 50 µL culture was whole slide imaged with a Axio Observer (Zeiss, Germany) equipped with an automated XY stage, generating a mosaic of phase contrast images. The mosaic was analyzed with an ImageJ plugin designed for automated analysis of *Streptomyces* pellets. Morphological details were analyzed using the Feret length of the particles and the morphology number which was calculated according to:

$$\frac{2\cdot\sqrt{A}\cdot S}{\sqrt{\pi}\cdot D\cdot E}$$

with A being the area of the particle, *S* the solidity, *D* the Feret length and *E* the aspect ratio (Wucherpfennig *et al.*, 2011). Further data analysis, construction of histograms and fitting of Gaussian curves were performed with Python (v3.3.2) and the sklearn library.

RESULTS

Growth and rheological characteristics of S. lividans 66 and its matAB mutant

For the duration of a batch cultivation, the majority of *S. lividans* 66 biomass occurs as pellets. In previous work we showed the benefits for growth when the main phenotype is shifted towards an open or dispersed phenotype (van Dissel *et al.*, 2015). In this study the effects of the morphology on the rheology were assessed, to determine whether it is feasible to further improve the fermentability of *S. lividans*. For filamentous fungi it is known that there is a gap between the effects of pelleting and a dispersed phenotype on the apparent viscosity of a culture (Kim *et al.*, 1983). Although the same morphology dependence was assumed for streptomycetes, there is only little experimental data available to support this hypothesis. Therefore, the difference between *S. lividans* and its *matAB* mutant was assessed in terms of morphology and rheology, in a biomass-dependent manner. Overnight cultures of these strains grown in TSBS media were concentrated by centrifugation and resuspension in fresh media and the viscosity was determined over a range of shear rates and biomass concentrations. With a good fit for the Ostwald-de Waele power law model, the broth of the *matAB* mutant showed strong non-Newtonian characteristics, even at low biomass concentrations (Figure 1). Up to a concentration of 8 g/L pellets did not yet have a major impact on the apparent viscosity. Once the biomass increased further it attained non-Newtonian characteristics, as observed by the dropping flow behavior index (Figure 1). These results revealed a big gap between the morphological phenotypes and their effect on the viscosity, which leaves room to further improve *S. lividans* fermentability.

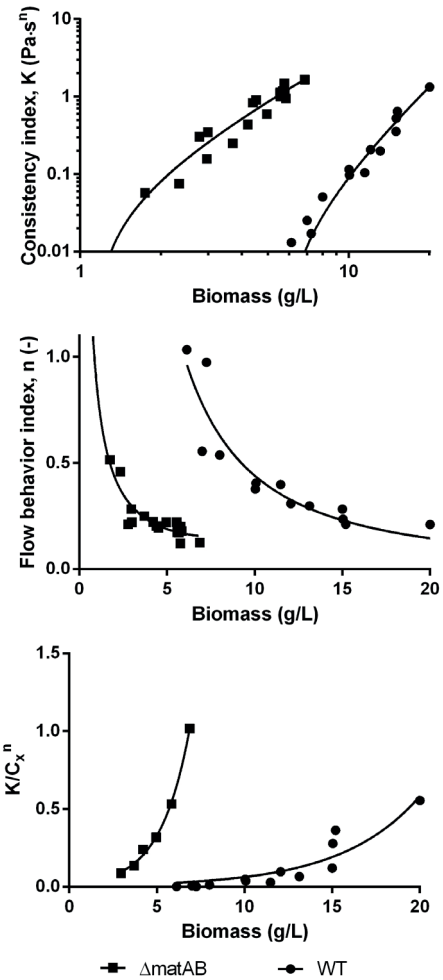

Figure 1. Rheology of S. lividans 66 its matAB null mutant. Cultures of *S. lividans* 66 (wild type; closed circles) and its *matAB* null mutant (closed squares) grown for 24 h were concentrated and the viscosity was determined for a serial dilution of the broth. The viscosity was used to calculate the parameters of the power law, revealing large rheological differences between two strains.

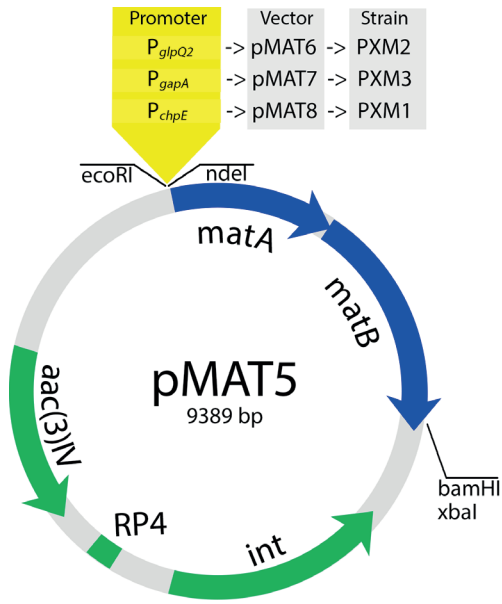

Figure 2. Map for the vectors with the matAB locus under the control of selected promoters.

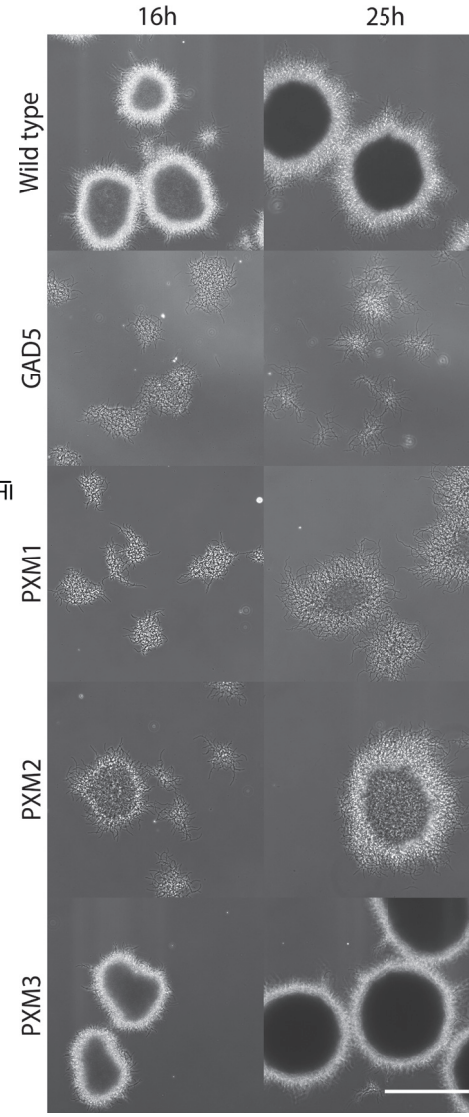

Figure 3. Mycelial morphology during early and late exponential growth. S. lividans 66 (Wild type), GAD5 (*ΔmatAB*), PXM1 (GAD5 + pMAT6), PXM2 (GAD5 + pMAT8) and PXM3 (GAD5 + pMAT7) were grown in a small benchtop bioreactor on TSB medium and sampled during the exponential growth curve. Overview microscope pictures were taken at 18 h and 25 h representing morphology during and late in the exponential growth phase respectively. The scale bar equals 500 µm.

Selection of promoters with favorable growth characteristics

Efficient mixing of nutrient and transfer of heat and gasses are highly dependent on the viscosity. In view of the trade-off between growth rate and rheology as a function of dispersed or aggregated growth, strain optimization approaches should consider a morphological profile that optimally profits from the advantages of dispersed mycelia (faster growth) and pellets (lower viscosity). To allow later expression of *matAB,* and hence delay production of the pellet-promoting PNAG, vectors were designed that allowed transcription of the *mat* locus from late promoters, and these constructs were then introduced into the *matAB* null mutant. The promoter regions of *chpE* and *glpQ2* were selected based on previously published timecourse transcriptomic data (Nieselt *et al.*, 2010). The *chpE* gene is developmentally controlled (Claessen *et al.*, 2003), resulting in low

transcription at the start of cultivation, but its transcription increases significantly towards the end of an exponential growth curve, with a peak at the onset of the stationary phase (Figure S1, data from GEO GSE18489 and (Thomas *et al.*, 2012)). The *glpQ2* gene is regulated through the *phoP* regulon, making it dependent on the phosphate concentration (Nieselt *et al.*, 2010). This gene is poorly expressed until the metabolic switch, at which point it is upregulated several folds (Nieselt *et al.*, 2010). As control the *gapA* promoter region was, which is expressed strongly throughout growth ((Zacchetti *et al.*, 2016) and Figure S1). Each of the promoters was cloned upstream of *matAB* in pSET152, which integrates in the *Streptomyces* chromosome (Bierman *et al.*, 1992). For a map of the plasmids see Figure 2. The plasmids were introduced into *S. lividans matAB* null mutant GAD5, creating PXM1 (GAD5 + pSET152-P^{chpE} *matAB*), PXM2 (GAD5 + pSET152-P^{glpQ2}*matAB*) and PXM3 (GAD5 + pSET152-P^{gapA}*matAB*).

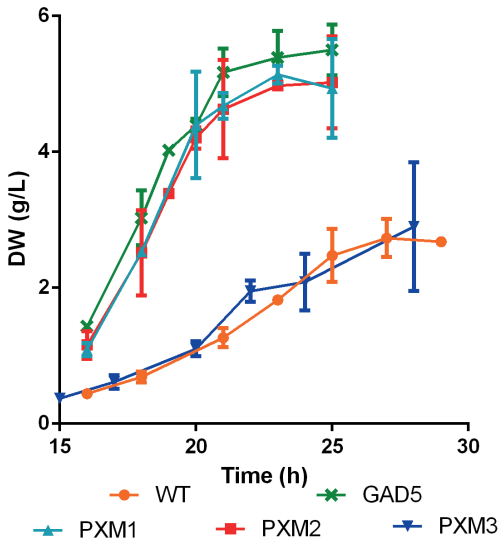

Figure 4. Growth curves of batch fermentations. Dry weight measurements taken during batch growth on TSB medium of all strains in small benchtop bioreactors. For strains see legend to Figure 3. Values represent the average of two experiments, with the error bars representing the deviation of the mean.

Variable matAB expression maintains fast growth with partial pellet formation

To assess their morphological behavior in relation to the parental strain and its *matAB* mutant, the transformants were batch-cultivated in a small benchtop bioreactors and the morphology and rheology determined over time. During cultivation the majority of the wild-

Table 1. Comparison of fermentation characteristics.

	Max Growth rate	Mean particle size #			Morphology Number #		
		16h	20h	25h	16h	20h	25h
Wild type	0.19 ± 0.01 h^{-1}	320 µm	439 µm	518 µm	0.61	0.58	0.62
GAD5	0.34 ± 0.01 h^{-1}	103 µm	127 µm	91 µm	0.13	0.18	0.13
PXM1	0.35 ± 0.01 h^{-1}	169 µm	253 µm	264 µm	0.21	0.33	0.36
PXM2	0.35 ± 0.01 h^{-1}	196 µm	258 µm	243 µm	0.38	0.33	0.34
PXM3	0.19 ± 0.01 h^{-1}	325 µm	419 µm	521 µm	0.62	0.71	0.67

The averages correspond to the right fitted Gaussian curve for the particle size and the Morphology Number as found in Figure 5 and 6 respectively.

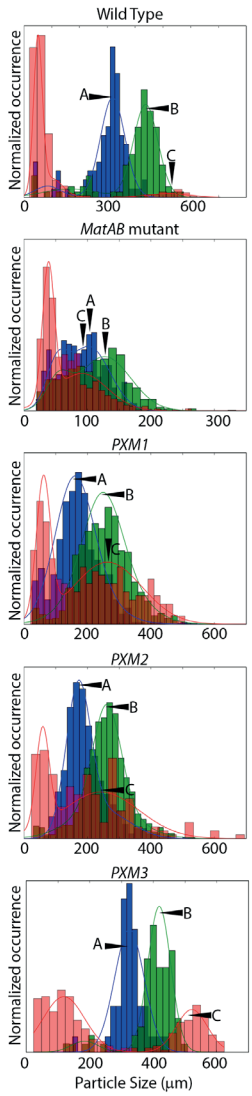

Figure 5. Particle size distribution of the fermentation at 16h, 20h and 25h. The maximum Feret length of particles were measured by image analysis for wild type S. lividans 66 the matAB null mutant GAD5, and transformants PXM1, PXM2, and PXM3 expressing matAB from the chpE, glpQ2 and gapA promoters, respectively. Times were 16h (blue), 20h (green) and 25h (red). Arrows indicate the primary peak of the pellet population, with A for 16h, B for 20h and C for 25h time points (values listed in Table 2). All strains had a large subpopulation of very small mycelial fragments at 25h. Two- component Gaussian curves were fit onto the raw data to estimate the average particle morphology number of multiple possible sub-populations of pellets and fragments.

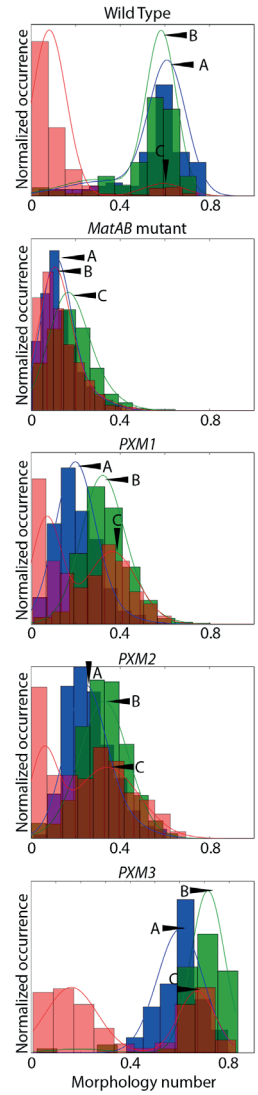

Figure 6. Morphology number distributions. Morphology numbers for S. lividans 66, GAD5, PXM1, PXM2 and PXM3 were determined after at 16 h (blue), 20 h (green) and 25 h (red). Calculations were done as described (Wucherpfennig et al., 2011). Two-component Gaussian curves were fit on the raw data to estimate the mean of particle morphology number of multiple possible sub-populations of pellets and fragments (triangles with A for 16 h, B for 20 h and C for 25 h). Values are summarized in Table 2.

type population consisted of pellets, while the *matAB* mutant had a characteristic dispersed morphology (Figure 3). The maximum growth rates were 0.19±0.01 h^{-1} for the parent and 0.34±0.01 h^{-1} for its *matAB* mutant (Figure 4 and Table 1), in line with earlier observations (van Dissel *et al.*, 2015).

16 h after inoculation, strains expressing *matAB* under the control of the developmentally controlled P^{chpE} or P^{glpQ2} promoters formed open clumps, which is intermediate between the morphologies of *S. lividans* 66 and its *matAB* mutant. After 25 h of growth the clumps had increased in size and density, forming what is best described as fluffy pellets, although more open clumps were also still part of the population (Figure 3). Importantly, biomass accumulation was similar to that of the *matAB* mutant, with a maximum growth rate of 0.36±0.01 h^{-1} and 0.35±0.01 h^{-1} for PxM1 and PxM2, respectively (Table 1). Conversely, transformant PXM3, which expresses *matAB* from the constitutive *gap* promoter, formed dense pellets and had a growth rate of 0.19 h^{-1}, similar to the parental strain.

The population dynamics over time were then quantified via image analysis. Previous studies used the maximum particle size to describe the morphology distribution found in submerged cultures (Martin & Bushell, 1996, O'Cleirigh *et al.*, 2005, Hobbs *et al.*, 1989). This allows describing the balance between growth and fragmentation. One or two Gaussian curves were fit through the distribution data to describe the particle distribution (Figure 5). Depending on the population, as a combination of spore aggregation, growth and fragmentation, two sub-populations were apparent, which are best described as two separate Gaussian curves (van Veluw *et al.*, 2012). The population with particle sizes below 100 µm primarily consists of sheared fragments and clumps while the other population consists of larger pellets. The maximal particle size for PXM1 and PXM2 cultures after 16 h of growth measured as the Feret diameter, was 169 µm and 196 µm, respectively (Table 1). This is an increase of 1.5-fold for PMX1 and of 2-fold for PMX2 in comparison to the *matAB* mutant. Between 16-20 h the Ferret diameter increased further for PXM1 and PXM2 to an average of 253 µm and 258 µm, respectively, while the diameter of the *mat* null mutant only increased minimally (to 127 µm) and in fact decreased by the end of exponential growth phase to an average value below 100 µm. At 25 h the average particle size of PXM1 and PXM2 had increased to around 300 µm indicating that aggregation was still progressing. This was still significantly smaller than the average pellet size found for the wild-type strain, which showed averages ranging from 320 µm at 16 h, 439 µm at 20 h and 518 µm at 25 h. This is comparable to transformant PXM3 (325 µm, 419 µm and 521 µm at 16 h, 20 h, and 25 h respectively).

Apart from the maximal particle size, image analysis also allowed the characterization of the morphology based on other visual characteristics. In an earlier study with the filamentous fungus *Aspergillus niger* the ratio of the area and solidity over pellet length and aspect ratio was used to describe the morphology and was named the Morphology Number (Wucherpfennig *et al.*, 2011). This ratio could also be used to describe the morphology of *Streptomyces* mycelia, with small fragments and open mycelia having a value close

to zero and pellets a value approaching one (Figure 6). Similar to manual morphological observations, PXM1 and PXM2 showed values for the morphology number in-between those of *S. lividans* 66 and its *matAB* mutant. PXM3 had a morphology number close to, but slightly higher than wild type, indicating that it aggregated to a higher degree that wild type. Interestingly, the morphology number for the parental strain remained roughly constant over time, indicating that the morphology of pellets in these cultures is stable. Otherwise the morphology number of PXM1 and PXM2 increased over time, indicating a gradual transition to pellet growth, although not to the same extent as the wild-type strain.

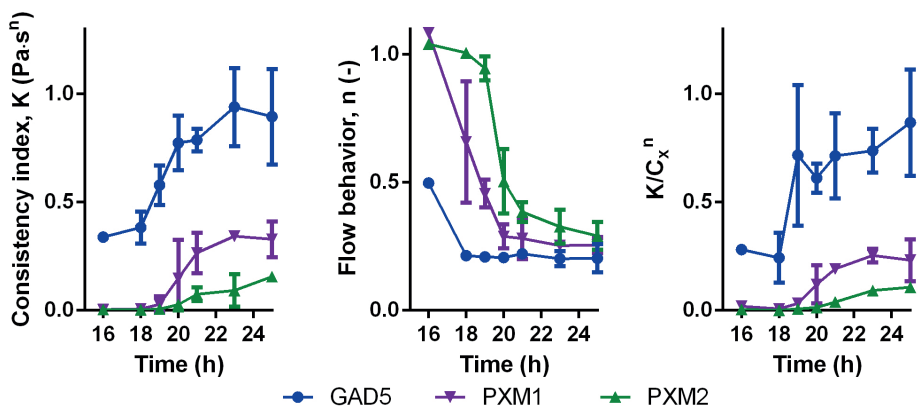

Figure 7. Change of rheology during the batch phase. During the exponential growth phase of GAD5, PXM1 and PXM2 samples were taken for offline viscosity measurments allowing the rheological characterization of the strains over time. Reological determination of wild-type *S. lividans* 66 and the PXM3 strains were outside the measurment range and were therefore not included. The apparent viscosity determined over a range of shear rates allowed fitting of the Ostwald–de Waele power law model. The values for consistency index K, the flow behaviour index n and the values related to the biomass K/C^n are depicted from left to right. Strains with late *matAB* expression showed superior rheological characteristics as compared to the *matAB* null mutant.

Rheological profile

The variation in broth rheology for all strains is presented in Figure 7. *S. lividans* 66 was not included in the comparison because the biomass concentrations remained below the threshold required to allow accurate measurement with a viscometer, with hardly any effect on rheology (Figure 2). Also PXM3, with a morphology similar to wild type, maintained a broth viscosity below the measurement range for the duration of the fermentation. Expectedly, both PXM1 and PXM2 showed a increased culture broth viscosity, but compared to the *matAB* null mutant both transformants showed a reduced average viscosity, illustrated by the consistency indices (K). And while PXM1 and PXM2 showed non-Newtonian characteristics by the end of the exponential growth phase, shown by the Flow behavior index (n), PXM1 and PXM2 attained these later than the *matAB* control strain. This is also reflected in the biomass-specific viscosity index (Riley *et al.*, 2000), which is

nearly 4 fold lower for PXM1 and about 8 fold lower for PXM2. Taken together, our data show that expression of the *mat* locus after initial growth resulted in improved rheological characteristics as compared to the *matAB* mutant, whilst maintaining a high growth rate.

DISCUSSION

Viscosity is one of the key limiting factors that dictates the efficiency of oxygen transfer during aerobic fermentations (Badino *et al.*, 2001). The entangling mycelium of streptomycetes and other filamentous micro-organisms can strongly increase the apparent viscosity, especially in low shear conditions because of the pseudoplastic behavior of the suspension. In many industrial scale fermentations the shear stress isn't that high, which, combined with a high viscose broth, results is a serious reduction of mass transport of among others oxygen (van't Riet & Tramper, 1991). Oxygen transfer suffers twice, because apart from elongated mixing times the higher viscosity increases the average bubble size, decreasing the oxygen transfer rate. As *Streptomyces* are aerobic micro-organisms that produce energy-expensive and thus oxygen-demanding natural products, maintaining a low viscosity should result in an improved process. Similarly, filamentous fungi that grow as pellets result in culture broths with low viscosity, which was for example beneficial for the production of lovastatin by *Aspergillus terreus* (López *et al.*, 2005). However, pellets are also associated with a low maximum growth rate, which extends fermentation times and thus increase operational costs. In particular the long fermentation times represent a bottleneck for *Streptomyces* as a production.

For filamentous fungi the morphology-associated rheology effects have been studied more extensively than for actinomycetes. Although many of the general trends are comparable, it appears that the biomass of *S. lividans* affects its environment differently. Comparing the dependencies of the flow behavior and biomass with values found for *Absidia corbymbifera* (Kim *et al.*, 1983), our work shows that both the dispersed mycelia and pellets of *S. lividans* have non-Newtonian behavior at much lower biomass concentrations than filamentous fungi. Interestingly, on average the consistency index was also lower, suggesting that the same biomass concentration has less effect on the viscosity. A plausible explanation could be sought in the difference at the cellular scale. The smaller *Streptomyces* hyphae are likely more fragile and thus more prone to fragmentation (Celler *et al.*, 2012). Cell damage caused by agitation already occurs at relatively modest agitation rates during *Streptomyces* fermentations (Roubos *et al.*, 2001, Heydarian *et al.*, 1999). Dispersed *Streptomyces* mycelia fragment more readily, resulting in smaller particle sizes and reduced entangling, with less effects on the viscosity. This effect of fragmentation is also visible for wild-type mycelia after 25 h, where numerous particles with a size <100 µm were found, supposedly originating from pellets that underwent fragmentation. It is unclear whether this fragmentation is the result of famine, which induces cell death (Manteca *et al.*, 2008) or the result of an increase in agitation rate required to meet the oxygen demand at the end of exponential growth. This requires further investigation.

To the best of our knowledge only one other study exists that attempted to rationally affect the morphology of a filamentous micro-organism to improve fermentation characteristics. Christian Müller and colleagues put *chsB* under the control of the *niiA* promoter in *Aspergillus oryzae* (Müller *et al.*, 2002b). The *chsB* mutant had an altered cell-wall architecture, showing hyper-branching and lack of pellets as compared to the parental strain (Müller *et al.*, 2002a). However, induction of *chsB* with the addition of nitrate did not result in the desired change in morphology. The positive effect of delayed expression of *matAB* in terms of improving the growth characteristics of *S. lividans* may be explained by the fact that altering *matAB* expression does not lead to radical changes in overall hyphal architecture, but rather to changes in the accumulated of the EPS-like PNAG, which acts as a 'glue' at the outside of the hyphae. In this sense *matAB* act very differently as compared to the *ssgA*, which has a major impact on hyphal differentiation, among others activating septum formation (Jakimowicz & van Wezel, 2012, Traag & Wezel, 2008). Overproduction of SsgA activates mycelial fragmentation in liquid-grown cultures, resulting in highly reduced particle size (van Wezel *et al.*, 2006). However, SsgA affects germination, tip growth, branching frequency and cell division (van Wezel *et al.*, 2000a, Noens *et al.*, 2007), which has major repercussions for hyphal integrity, among others leading to increased cell lysis.

It is currently unclear why late expression of *matAB* only resulted in less dense pellets, instead of fully mature pellets. Perhaps delayed production of PNAG is insufficient for fully mature coalescence. Alternatively, the lack of PNAG during the earliest stages of growth may also affect spore aggregation, another important determinant of pellet morphology (Zacchetti *et al.*, 2016). Spore aggregation depends on *matAB* during germination and the first few hours of growth. Delaying *matAB* transcription during growth likely eliminates spore aggregation and will thus affect population dynamics. Aggregated spores may create a nucleation point for the complex scaffolding needed to form the dense core of pellets, and this will be different from later aggregation events as shown in this study.

Industrial fermentations are often conducted as fed-batch cultures, and the benefits of deregulation of *matAB* expression may be more beneficial in such a system. Studies into the rheology of fed-batch cultures established a further increasing apparent viscosity during the feeding stage, indicating that in fed-batch systems there is more to gain by controlling the morphology (Pamboukian & Facciotti, 2005). Expressing the *mat* locus in actinomycetes that do not have a copy of the *mat* genes on their chromosome and grow dispersed, exemplified by for example the clavulanic acid producer *Streptomyces clavuligerus* or the erythromycin producer *Saccharopolyspora erythraea*, typically induces the formation of mycelial pellets . We therefore expect that our work can be translated to many other systems, thus offering the outlook of tuning the rheology with the aim of improving the productivity of a range of fermentation processes involving filamentous *Actinobacteria*.

ACKNOWLEDGEMENTS

We like to thank Joost Willemse for the support with the automated image analysis. The research was supported by VICI grant 10379 from the Netherlands Technology Foundation STW to GVW.

SUPPLEMENTAL INFORMATION

Table S1: Oligonucleotides

Primer name	Sequence
SCO2963_F	CAGTGAATTCCATATGGGGGCCGGTTCGGCCGACGAGTGCTC
SCO2962_R	ATGCGGATCCTCATCCGACCGGCCTCCCGTCCATGGC
pSCO1800_F	AGTGAATTCCCGTCCACGCCGGGCACATC
pSCO1800_R	AGTCATATGCAACCCCTCCTTGCGATCGCC
pSCO1947_F	AGTCGAATTCATCGCGTACGTCACCGACCC
pSCO1947_R	AGTCCATATGCCGATCTCCTCGTTGGTACGCC
pSCO1968_F	GATGAATTCGGGCGCCAGGAACGGCTGAC
pSCO1968_R	GATCATATGTACTCCTCGCGTCGAACGAT

Table S2: Strains and vectors used in this study

Strain name	Genotype	Reference
S. lividans 66	SLP2+ SLP3+	(Kieser *et al*., 2000)
GAD5	*S. lividans* 66 ΔmatAB	(van Dissel *et al*., 2015)
PXM1	GAD5 + pSET152-P^{ChpE}-*matAB*	this study
PXM2	GAD5 + pSET152-P^{GlpQ2}-*matAB*	this study
PXM3	GAD5 + pSET152-P^{GapA}-*matAB*	this study

Vector name	Construct	Reference
pSET152	*oriT* RK2, pUC18 replicon, $Apra^R$	Bierman *et al*., 1992
pJET1.2	pUC18 replicon, Amp^R	CloneJET PCR cloning kit, Fermentas
pMAT5	pSET152-*matAB*	this study
pMAT6	pSET152-P^{glpQ2}- *matAB*	this study
pMAT7	pSET152-P^{gapA}- *matAB*	this study
pMAT8	pSET152-P^{chpE}- *matAB*	this study

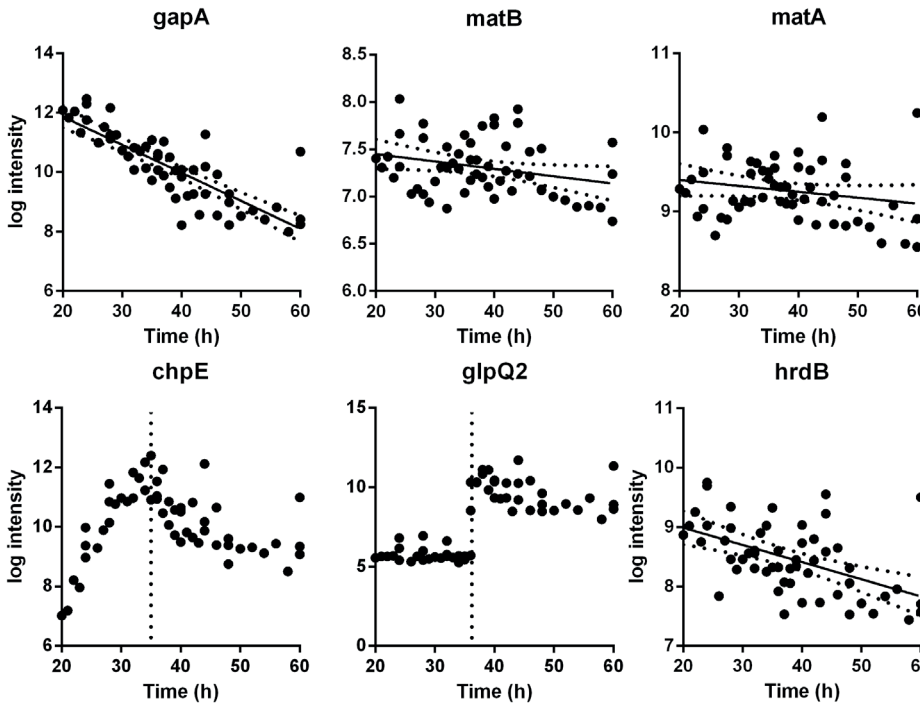

Figure S1: Expression data of gapA (SCO1947), matB (SCO2962), matA (SCO2963), chpE (SCO1800), glpQ2 (SCO1968) and hrdB (SCO5820) obtained from GEO GSE18489 and). Depicted here are the mRNA levels from high density sampling of batch fermentation with *Streptomyces coelicolor* performed by (Thomas *et al.*, 2012). From this data can be concluded that *gapA, matA* and *matB* have a constitutive expression pattern and the expression levels of *chpE* and *glpQ2* are low early during the batch phase, but increase over time. The principle vegetative sigma factor hrdB is depicted as example of a stable household gene.


5